Limnol. Oceanogr., 53(5), 2008, 1734–1745

Propagation of an atmospheric climate signal to phytoplankton in a small marine basin

William K. W. Li[1] *and W. Glen Harrison*
Bedford Institute of Oceanography, P.O. Box 1006, Dartmouth, Nova Scotia B2Y 4A2, Canada

Abstract

A 14-yr record of weekly observations in Bedford Basin (Canada) was used to describe the direction and magnitude of departures from long-term mean conditions in both climate and plankton components, for the purpose of detecting common patterns. Seasonal vertical stratification of the water column is determined primarily by temperature, but multiyear change in the annual deseasonalized average stratification is induced by salinity, which is linked to precipitation and river discharge. Stratification anomalies explain significant amounts of variability in the anomalies of nutrients and total phytoplankton biomass, especially that contributed by diatoms, but not the biomass of nanophytoplankton and picophytoplankton. Instead, the responses of the small phytoplankton groups appear directly related to temperature. Trophic linkage between phytoplankton and copepods is not statistically demonstrable, but there is strong evidence of linkage between phytoplankton and bacterioplankton. Temporal sign switching, which is the coherent departure from norm in both an ecosystem driver and response, strongly indicates the propagation of an atmospheric signal to phytoplankton in surface waters of Bedford Basin and thence further through trophic linkage and export.

In the North Atlantic, interannual climate variability is strongly influenced by recurrent redistribution of atmospheric mass between the Arctic and the subtropical Atlantic (Hurrell and Dickson 2004). Since the time and space scales of this climatic forcing are large, it can be surmised that ecosystem responses will be evident at commensurate scales, as indeed has been shown in multidecadal ocean basin studies (Parmesan and Yohe 2003). Nevertheless, climate effects are experienced at small scales through local influences of heat, wind, precipitation, cloud cover, and radiation (Miller and Harding 2007). The chaotic nature of weather means that local departures from the regional pattern are to be expected. Yet, there is a need to predict climate impacts in many particular inshore locations, often because of socioeconomic concerns. The difficulty of extracting a climate signal from coastal ecosystems is compounded by a multitude of coacting environmental stressors such as nutrient enrichment, fishing harvest, and toxic contaminants (Cloern 2001). To detect change at a single site, local observations must be made at frequent intervals over a long time. Such data can be rescaled to indicate interannual variations (Cullen et al. 2007, Li 2007) but difficulties remain in identifying mechanisms embedded within the climate driver actually responsible for observed changes (Smayda et al. 2004).

Phytoplankton are sentinels of environmental change because, as primary producers, their cellular rates of reproduction are directly determined by the abiotic environment. The annual cycle of phytoplankton development through the seasons is generally well understood, and useful typologies can be constucted on the basis of a small number of controlling factors such as vertical stability, nutrient supply, illumination, and grazing pressure (Longhurst 1995). The issue we address in this paper is the multiyear response of phytoplankton to environmental forcing. Thus we seek a signal that is embedded in strong repeating seasonal cycles, but that could be much less intense. A factor that dominates seasonal forcing cannot be assumed a priori to also be the driver of phytoplankton change from year to year. This is because both forcing and response return approximately to their initial states at the beginning of each annual cycle. Any long-term signal must necessarily be discerned as departures from the annual average state. The long-term response supersedes the timescales related to physiological reaction and population dynamics; therefore the effects are not proximal.

Here, we present a series of linked associations to suggest the possible processes by which a climate signal was apparently propagated to phytoplankton in a small marine basin. We show that annual changes in bulk phytoplankton biomass are strongly associated with diatoms that are sensitive to annual changes in stratification induced by salinity, even though the proximal determinant of stratification is temperature. The interannual responses of other phytoplankton groups appear more complex, being related to water temperature but not mediated through vertical mixing. Once multiyear climate signals are transmitted into the food web through phytoplankton, they may subsequently appear in other organismal groups by trophic linkage (Richardson and Schoeman 2004; Li et al. 2006*a*), further propagating the effects throughout the ecosystem.

Methods

Site description—Bedford Basin is the inner portion of Halifax Harbour on the Atlantic coast of Canada. The

[1] Corresponding author (LiB@mar.dfo-mpo.gc.ca).

Acknowledgments

We thank the following persons for technical contributions: Paul Dickie, Tim Perry, Kevin Pauley, Jeff Spry, Jeff Anning, Carol Anstey, Edward Horne, Marie-Hélène Forget, and several summer students. We also thank Brian Petrie for critical reading of an early version of the manuscript, and three anonymous reviewers for their diligent work.

Financial support was provided by Department of Fisheries and Oceans Strategic Science Fund in the Ocean Climate Program and the Atlantic Zone Monitoring Program.

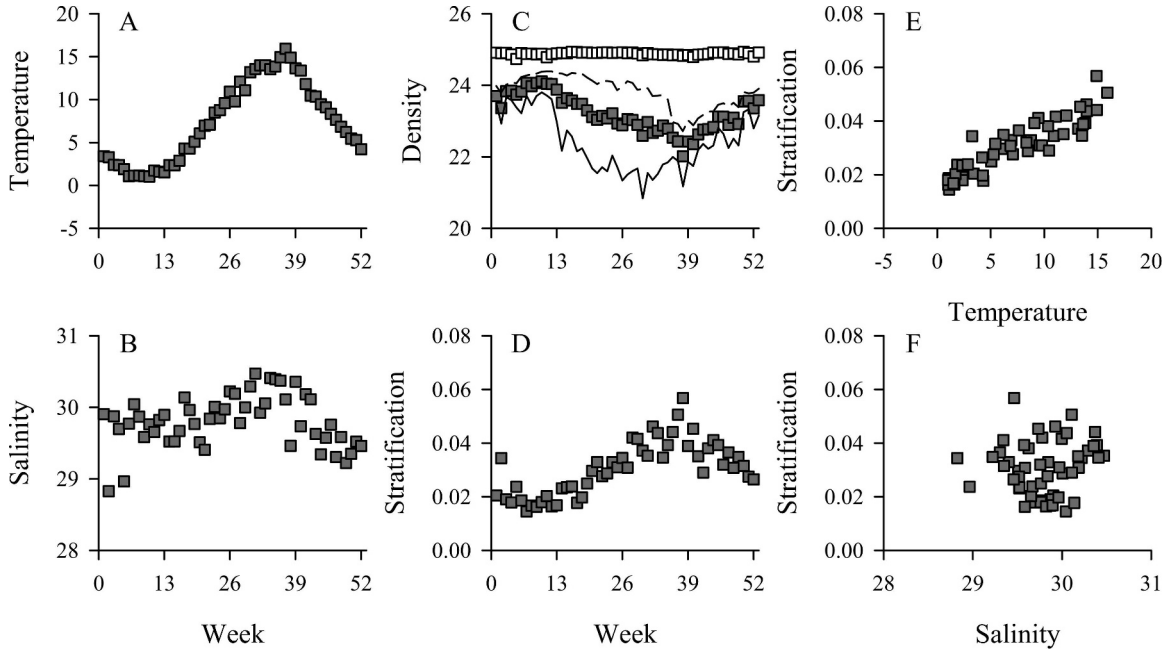

Fig. 1. Annual cycle of density stratification constructed from multiyear observations averaged into weekly bins. (A) Seawater temperature (°C). (B) Salinity. (C) Density σ_t (kg m^{-3}). (D) Stratification (kg m^{-4}). (E) Stratification vs. temperature. (F) Stratification vs. salinity. Filled symbols: average of measurements made at 1, 5, and 10 m. Open symbols: measurements made at 60 m. Solid line: measurements made at 1 m. Dashed line: measurements made at 10 m.

geographic, oceanographic, and hydrological description of the harbor is given in detail by Petrie and Yeats (1990) and by Gregory et al. (1993), from which we summarize as follows. The basin is an estuary with a surface area of 17 km^2, a volume of 5.1×10^8 m^3, a maximum depth of 71 m, and a connection to the adjoining continental shelf through a narrow (400 m) and shallow (20 m) sill. The basin receives freshwater from the Sackville River at an average inflow of 5 m^3 s^{-1}, a maximum of 12 m^3 s^{-1} in the spring and a minimum of 1 m^3 s^{-1} in the summer. Additional runoff enters the basin from the watershed, which has an area of 281 km^2. The mean circulation is a two-layer structure where lower-density surface water flows outward to the open Atlantic, and deeper saline water flows into the basin over the sill. The mean tidal range is 1.5 m, the ratio of tidal to freshwater volume is 109, and the flushing time is 261 h. From considerations of water exchange at the inlet mouth, the plankton in Bedford Basin are thought to lose their autonomy as an independent ecological unit when external physical forces dominate intrinsic biological dynamics at timescales longer than about 3 d (Lewis and Platt 1982).

Sampling—The compass buoy station (44°41′37″ N, 63°38′25″W) is in the deepest part (71 m) of Bedford Basin. Since 1993, it has been occupied almost every week, usually on Wednesday morning, by a small launch. Transit time from the institute pier to the station is about 15 min. Details of the sampling program have been published (Li and Dickie 2001). Briefly, a profiling conductivity–temperature–depth system records temperature, conductivity, in vivo fluorescence, and photosynthetically active radiation (PAR). Seawater samples are collected by Niskin bottle at 4 depths: 1, 5, 10, and 60 m. Mesozooplankton are collected using a 0.75-m ring net of 202-μm mesh size towed vertically at approximately 1 m s^{-1} from near bottom at about 65 m depth to the surface.

Data sources—The North Atlantic Oscillation (NAO) index was obtained from the Climate Analysis Section, National Center for Atmospheric Research, Boulder at http://www.cgd.ucar.edu/cas/jhurrell/indices.html. It is the winter (December through March) index of the NAO based on the difference of normalized sea level pressure between Lisbon, Portugal, and Stykkisholmur near Reykjavik, Iceland since 1864. Air temperature and preciptation data were recorded at Shearwater airport WMO id# 71601 (44°37′N, 63°30′W) and obtained from Environment Canada at http://www.climate.weatheroffice.ec.gc.ca/climateData/canada_e.html. Freshwater discharge from the Sackville River was recorded at Bedford (44°43′53″N, 63°39′45″W) and obtained from the National Water Quantity Survey program of Environment Canada at http://www.wsc.ec.gc.ca/hydat/H2O/.

Sample analysis—Details of analytical methods have been published (Li and Dickie 2001; Mitchell et al. 2002). Nutrients were frozen after collection, and subsequently measured by autoanalyzer. Particulate organic carbon (POC) was measured by Perkin Elmer Series II CHNS/O Analyzer 2400, but sampling for POC was initiated only in late 2002 so the time series is very short. Chlorophyll *a* (Chl *a*) was measured in acetone extracts of particulate matter collected on Whatman GF/F filters by in vitro fluorometric analysis using a Turner Designs fluorometer. In addition, Chl *a* and accessory phytoplankton pigments were also

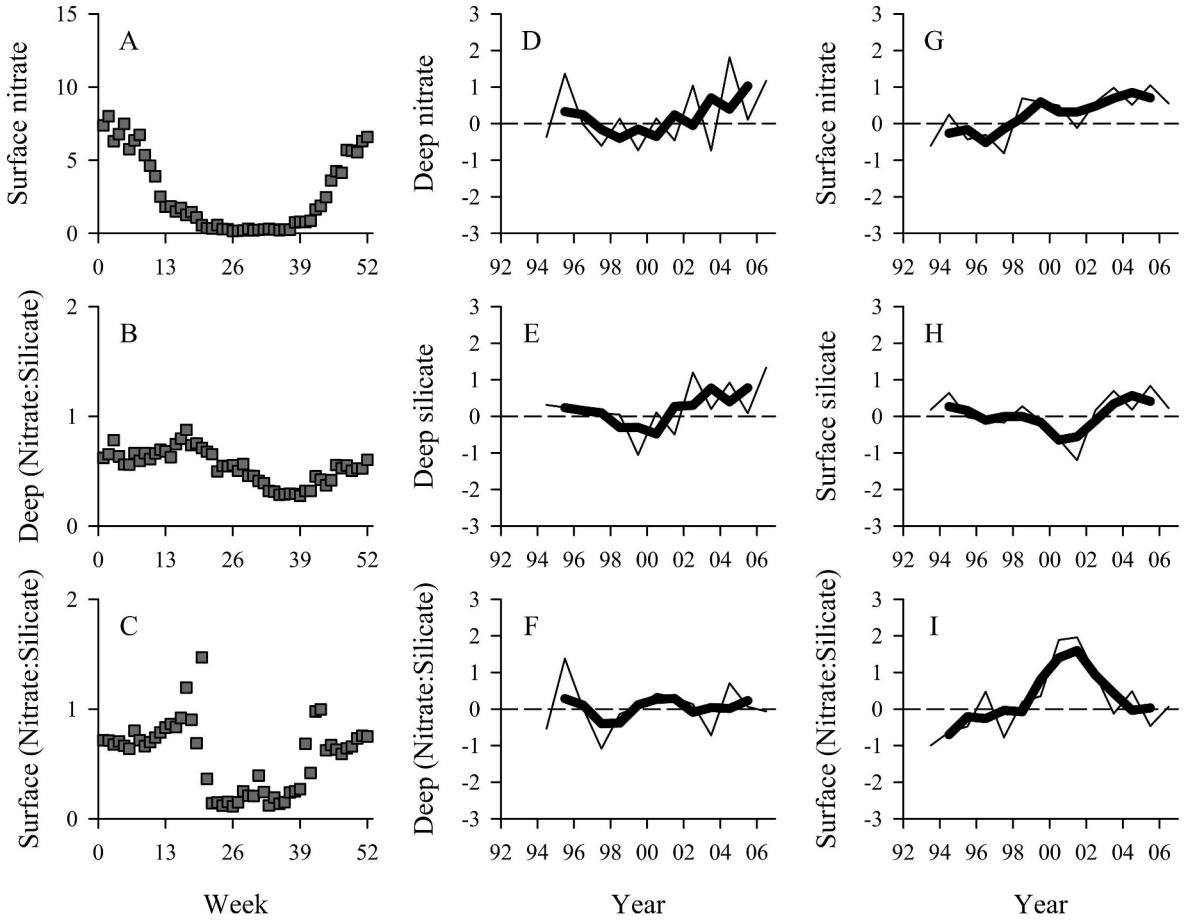

Fig. 2. Nitrate and silicate in surface (average of 1, 5, and 10 m) and deep (60 m) waters. (A) Annual cycle of surface nitrate concentration. (B) Annual cycle of deep nitrate : silicate. (C) Annual cycle of surface nitrate : silicate. (D) Time series of deep nitrate concentration. (E) Time series of deep silicate concentration. (F) Time series of deep nitrate : silicate. (G) Time series of surface nitrate concentration. (H) Time series of surface silicate concentration. (I) Time series of surface nitrate : silicate. Thin solid line is normalized annual anomaly, thick solid line is three-point running average, dashed line indicates normal conditions from 1993 to 2000.

measured by high-performance liquid chromatography (HPLC) on particulate matter collected by filtration and stored frozen at −80°C (Bouman et al. 2003). The sum of seven diagnostic accessory pigments (19′-butanoyloxyfucoxanthin, 19′-hexanoyloxyfucoxanthin, fucoxanthin, alloxanthin, chlorophyll *b*, zeaxanthin, and peridinin) is strongly correlated with total Chl *a*, and is an alternate index of phytoplankton biomass (Claustre 1994). Recognizing that not all of these pigments are absolutely diagnostic (Jeffrey and Vesk 1997), we nevertheless follow current convention of large-scale studies (Uitz et al. 2006) in using fucoxanthin as a biomarker for diatoms, and peridinin for dinoflagellates. The proportion of phytoplankton biomass that is contributed by diatoms is estimated by the ratio (1.41 × fucoxanthin) : Chl *a* (Uitz et al. 2006). In our study area, the general form of the annual cycles in diatoms and dinoflagellates (Li et al. 2006*b*) match those in fucoxanthin and peridinin, respectively. The sum of the remaining five diagnostic pigments (here designated P5) represents a functional group of small phytoplankton consisting of nanoflagellates, picoflagellates, and picocyanobacteria generally associated with regenerated production (Claustre 1994).

Picophytoplankton, nanophytoplankton, and bacterioplankton were collected in seawater aliquots, dispensed into cryogenic vials, fixed in 1% paraformaldehyde, stored frozen at −80°C, and subsequently counted by flow cytometry (Li and Dickie 2001). Biovolumes of picophytoplankton (<2 μm), small nanophytoplankton (2–10 μm), and large nanophytoplankton (10–20 μm) estimated from the measured size spectra (Li and Dickie 2001) were converted to carbon biomass using the factors 0.36, 0.24, and 0.16 pg μm^{-3} C respectively for the three size classes (Verity et al. 1992). As a unit, this community of small phytoplankton may be characterized by a macroscopic property, which is the assemblage mean cell size. This quantity is calculated as the equivalent spherical diameter (ESD) of the average biovolume, representing the abundance-weighted distribution of biovolume in a spectrum of graded-size bins (Li and Dickie 2001).

Mesozooplankton were counted and weighed as described in Mitchell et al. (2002) and indexed as $\log_{10}(Z + 1)$ where Z is the number or wet weight of animals per square meter. Nil counts of Z return an index value of 0. To date, samples have been processed only for the 5-yr period 1998–2002.

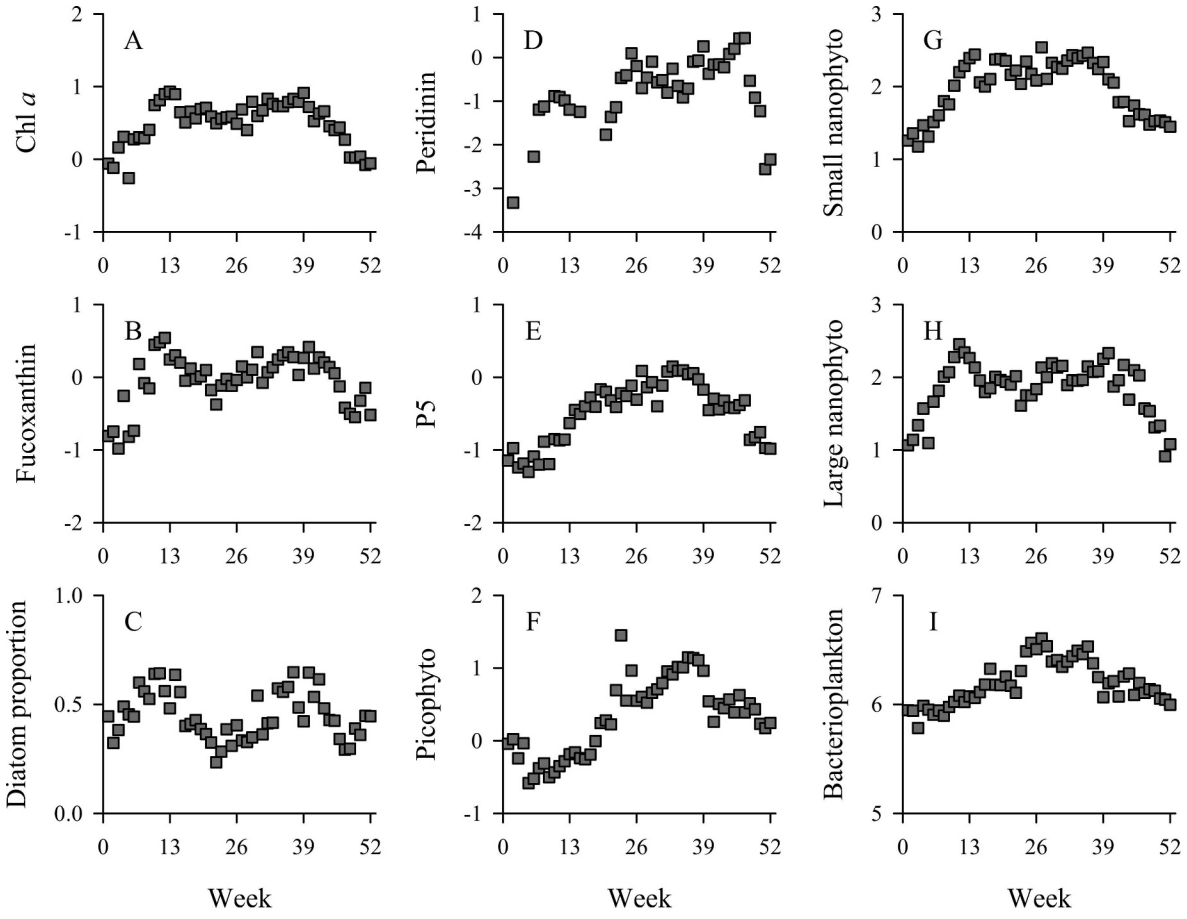

Fig. 3. Annual cycles of microbial plankton constructed from multiyear observations averaged into weekly bins. (A) Chl *a* (log mg m^{-3}). (B) Fucoxanthin (log mg m^{-3}). (C) Diatoms as a proportion of phytoplankton, *see* Methods. (D) Peridinin (log mg m^{-3}). (E) P5, *see* Methods (log mg m^{-3}). (F) Picophytoplankton (log mg C m^{-3}). (G) Small nanophytoplankton (log mg C m^{-3}). (H) Large nanophytoplankton (log mg C m^{-3}). (I) Bacterioplankton (log cells ml^{-1}).

Data analysis—Separate results from the analysis of samples collected at 1, 5, and 10 m were averaged to give a single composite surface value for Chl *a*, nitrate, phosphate, silicate, accessory photosynthetic pigments, and bacterioplankton. For picophytoplankton, nanophytoplankton, and POC, data were available only at 5 m to represent surface values. Deep values were taken from 60-m samples. Vertical stratification of the water column (kg m^{-4}) was calculated as the depth-normalized difference of seawater density between deep (60 m) and shallow (average of 1, 5, and 10 m) waters, ensuring a match between the description of physical and biological stratification. Light attenuation coefficient was calculated as the rate of exponential decay of measured PAR with depth, from 1 to ca 10 m.

The normal baseline period for most measurements was defined as the years up to and including 2000 for which data are available. This follows standard convention of the World Meteorological Organization wherein current world climate normals are defined using the 30-yr period 1971–2000 (www.climate.weatheroffice.ec.gc.ca). Over this period, each week in the 52-week cycle has eight or fewer observations, one from each year since monitoring began, and the average of these constitutes the norm for that week. For each variable, the difference between observed value and the normal value at a given week is the anomaly. Dividing the anomaly by the week-appropriate standard deviation gives the standard anomaly. The average of 52 such values in a year gives the normalized annual anomaly. An example of this calculation is illustrated by Cullen et al. (2007) for the picoeukaryotic phytoplankton in Bedford Basin. This final quantity expresses the deviation of any variable from its norm in standard deviate units. Following standard convention in oceanic hydrographic climatology (Hughes and Holliday 2007), we use this quantity (normalized annual anomaly) as the basis for common comparison and rank correlation across all variables in this paper. The observations for POC and mesozooplankton only span a short period ($\leq$5 yr) so climate normals were calculated using the entire available time series.

Pairwise nonparametric association of normalized annual anomalies (running average) was tested using Kendall's coefficient of rank correlation (τ), and judged for significance using a table of critical values as a test for zero slope. Kendall's robust line fit method for estimating the median slope and intercept of the association was

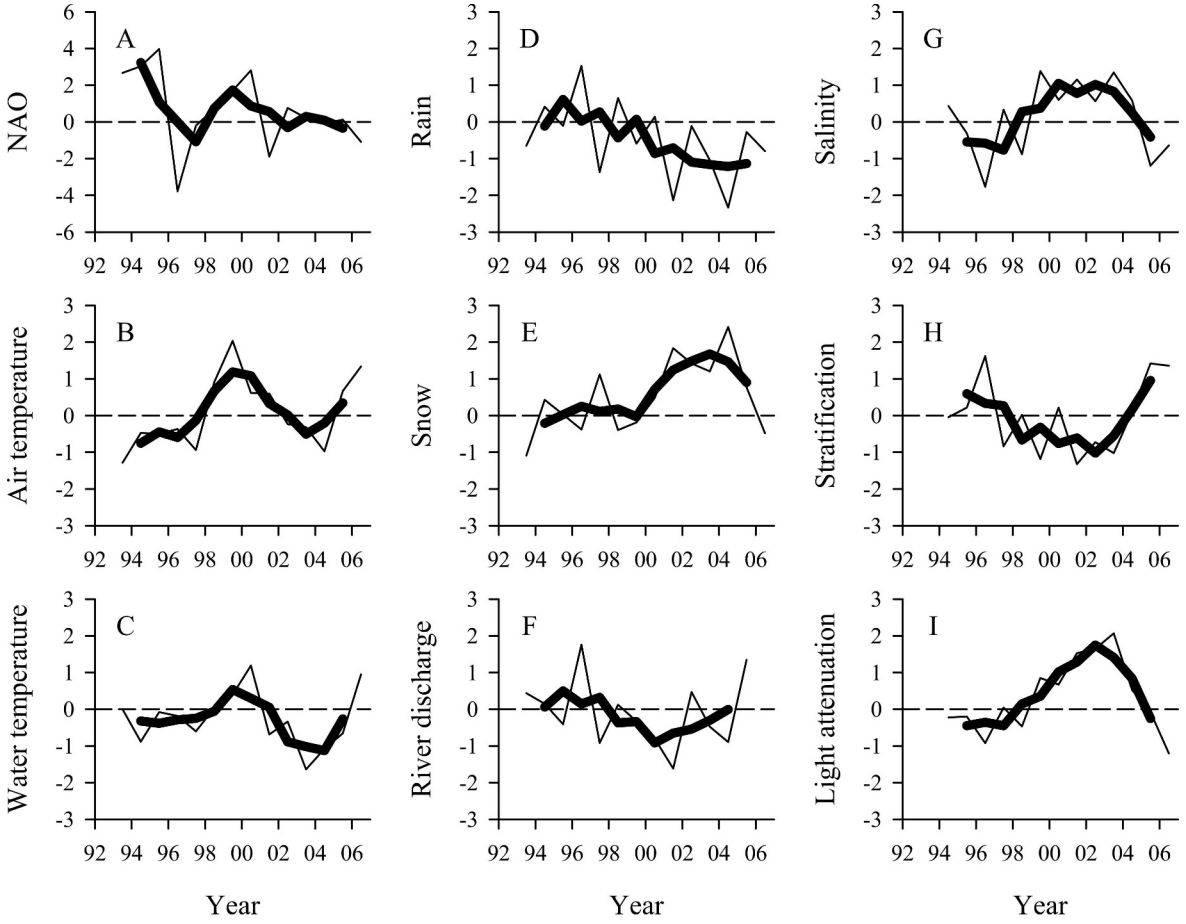

Fig. 4. Time series of meteorological, hydrological, and optical measurements. (A) North Atlantic Oscillation index. (B) Air temperature (°C). (C) Surface seawater temperature (°C). (D) Rain (mm). (E) Snow (cm). (F) River discharge ($m^3\ s^{-1}$). (G) Surface salinity. (H) Vertical stratification ($kg\ m^{-4}$). (I) Light attenuation coefficient (m^{-1}). Lines as in Fig. 2.

performed by software implementation (BIOMstat) of Sokal and Rohlf (1995).

Results

The normal state—Seasonal vertical stratification is primarily determined by temperature and not by salinity, as evident by the annual cycle of surface seawater density, which is at its lowest point in late summer when temperature is highest, and in spite of high salinity (Fig. 1). Weekly average values of stratification are highly correlated with temperature (Fig. 1E, $r = 0.90$, $p < 0.001$) but not with salinity (Fig. 1F, $r = 0.10$, $p = 0.46$). In a multiple regression of temperature and salinity on stratification, the Kruskal index of importance (Sokal and Rohlf 1995) is higher for temperature (0.89) than for salinity (0.40). Nitrate is depleted in surface waters throughout summer (Fig. 2A), and the nitrate : silicate ratio rarely exceeds 1 any time of year in either the deep source water (Fig. 2B) or the surface water (Fig. 2C) in which the nutrients are assimilated by phytoplankton.

Total phytoplankton biomass (Fig. 3A) is maximum in the spring during the period of weakest stratification, but is sustained at high levels throughout the summer and into the autumn during periods of high temperature. Diatoms (Fig. 3B) also bloom in the spring and autumn, representing 65% of the phytoplankton biomass at these peak times (Fig. 3C). Dinoflagellates peak in late autumn (Fig. 3D). The functional group consisting of nanoflagellates, picoflagellates, and picocyanobacteria has an annual cycle (Fig. 3E) somewhat similar to that of temperature ($r = 0.77$, $p < 0.001$). Within this group of small cells, picophytoplankton (Fig. 3F) track the temperature cycle with much similitude ($r = 0.90$, $p < 0.001$), whereas nanophytoplankton (Fig. 3G,H) do not because of a conspicuous spring bloom. Since seasonal stratification is primarily determined by temperature, picophytoplankton are also highly correlated with stratification within the annual cycle ($r = 0.80$, $p < 0.001$). Bacterioplankton peak at almost exactly mid-year, but are sustained at high levels throughout the summer (Fig. 3I).

Stratification anomalies—To discern multiyear trends of change, we deseasonalize the data (*see* Methods) so that patterns linking environment to phytoplankton at the intra-annual scale are removed. At the interannual scale, the NAO (Fig. 4A) is the prevalent climate driver over much of the North Atlantic (Hurrell and Dickson 2004), but local

Table 1. Rank correlation testing for the significance of nonparametric association between pairs of variables (normalized annual anomalies) on the basis of Kendall's robust line fit giving the median slope and intercept, where n is the number of data pairs, τ is the coefficient of rank correlation, and p is the probability level, where values >0.10 are deemed not significant (ns).

Figure	*X*	*Y*	Slope	Intercept	*n*	Kendall's τ	*p*	
5A	Precipitation	River discharge	0.56	0.10	12	0.52	<0.05	
5B	River discharge	Salinity	−1.41	−0.13	10	−0.69	<0.01	
5C	Salinity	Stratification	−0.72	−0.05	11	−0.60	<0.01	
5D	Temperature	Stratification	−0.20	−0.20	11	−0.16	>0.10	ns
5E	Stratification	Delta nitrate	0.39	0.22	11	0.49	<0.10	
5F	Stratification	Chl *a*	−0.63	0.26	11	−0.49	<0.10	
5G	Stratification	Fucoxanthin	−0.90	0.00	10	−0.78	<0.01	
5H	Stratification	Surface (nitrate : silicate)	−0.70	0.20	11	−0.45	<0.10	
5I	Stratification	Light attenuation	−1.01	0.25	11	−0.56	<0.05	
–	Stratification	Peridinin	−0.78	−0.46	10	−0.29	>0.10	ns
7A	Stratification	P5	−0.15	0.34	10	−0.02	>0.10	ns
7B	Water temperature	P5	−0.86	0.33	10	−0.56	<0.05	
7C	Water temperature	Assemblage mean ESD	−1.22	−0.17	12	−0.73	<0.01	
7D	Water temperature	Large nanoplankton carbon	−0.86	−0.20	12	−0.67	<0.01	
7E	Water temperature	Small nanoplankton carbon	−0.68	−0.05	12	−0.33	>0.10	ns
7F	Water temperature	Picoplankton carbon	0.60	−0.26	12	0.48	<0.05	
7G	Chl *a*	Bacterioplankton	0.87	0.59	10	0.69	<0.01	
7H	Chl *a*	Deep Chl a	0.80	0.28	11	0.64	<0.01	
7I	Stratification	Deep POC	−0.65	0.41	4	−0.67	>0.10	ns
8G	Chl *a*	Mesozooplankton wet weight	0.88	0.38	5	0.60	>0.10	ns
8H	Chl *a*	*Oithona similis*	0.56	0.23	5	0.40	>0.10	ns
8I	Chl *a*	*Pseudocalanus spp.*	0.62	0.26	5	0.40	>0.10	ns
–	Chl *a*	*Acartia clausi*	0.46	−0.28	5	0.20	>0.10	ns
–	Chl *a*	*Eurytemora herdmani*	1.32	−3.47	5	0.40	>0.10	ns
–	Chl *a*	*Temora longicornis*	−0.11	0.78	5	0.00	>0.10	ns

air temperature (Fig. 4B) appears uncoupled from this large-scale forcing. Local air temperature is significantly rank correlated ($\tau = 0.55$, $p < 0.05$) with surface water temperature in Bedford Basin (Fig. 4C), suggesting effective local heat transfer. Yet, in Bedford Basin, at the interannual scale, stratification is controlled by salinity rather than temperature (Kruskal's index of importance = 0.77 and 0.03 respectively), exactly opposite to the control of stratification at the intra-annual scale described in the previous section. Annual changes in salinity (Fig. 4G) mirror those in river discharge (Fig. 4F), which depend on rain (Fig. 4D) and snow (Fig. 4E). The time series of stratification anomalies (Fig. 4H) is essentially a mirror of salinity anomalies (Fig. 4G).

When surface waters became more saline in 1998–2004, stratification was reduced. A sequence of rank correlations (Table 1) suggests how the signal might have been propagated. Less precipitation decreased river discharge (Fig. 5A); less river discharge increased surface salinity (Fig. 5B); higher salinity decreased stratification (Fig. 5C); and weak stratification reduced the difference between deep and surface nitrate concentrations (Fig. 5E). At the interannual scale, temperature and stratification are not correlated (Fig. 5D).

Microphytoplankton anomalies—The years of weak stratification were the years of high phytoplankton biomass (Fig. 6A), particularly from the contribution of diatoms (Fig. 6B). The strength of the rank correlation between stratification and fucoxanthin (Fig. 5G, Table 1) exceeds that between stratification and Chl *a* (Fig. 5F), indicating that diatoms were more responsive to stratification effects than other phytoplankton. Notably, peridinin (Fig. 6C) is not statistically correlated with stratification (Table 1), suggesting that dinoflagellate motility might be effective against the stratification barrier to nutrient availability.

All phytoplankton require nitrogen as an essential macronutrient, but diatoms are the only major group that also requires silicon in approximately equimolar amounts. A diatom-dominated community therefore imparts a signature of high residual N : Si ratio in its suspending mileu. The nutrient ratio in deep water has not changed substantially for many years (Fig. 2F), but the surface water shows evidence of extra Si demand during the years of above-average diatom abundance (Fig. 2I). An inverse correlation between anomalies of stratification and N : Si in surface water (Fig. 5H) is consistent with a diatom signature.

Picophytoplankton and nanophytoplankton anomalies—In recent years, the taxonomically diverse group of phytoplankton P5 has increased in biomass (Fig. 6D) because of above-normal nanophytoplankton (Fig. 6F,G) and in spite of below-normal picophytoplankton (Fig. 6E). Notably, the change is not significantly related to stratification (Fig. 7A). Instead, P5 is negatively associated with water temperature (Fig. 7B). Mean cell size of these small phytoplankton is also inversely related to temperature (Fig. 7C), reflecting a strong weighting of the large nanophytoplankton component (Fig. 7D). Picophyto-

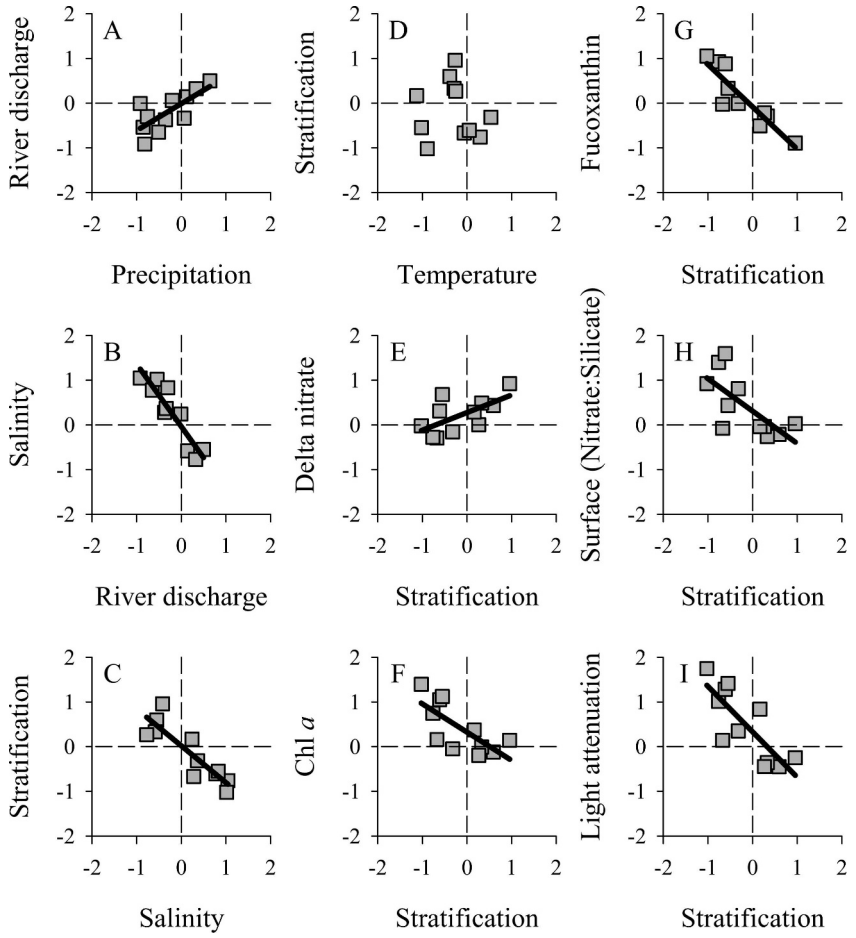

Fig. 5. Rank correlations of normalized annual anomalies. (A) Precipitation vs. river discharge. (B) River discharge vs. salinity. (C) Salinity vs. stratification. (D) Temperature vs. stratification. (E) Stratification vs. the difference in nitrate concentration between deep and surface water. (F) Stratification vs. log Chl *a*. (G) Stratification vs. log fucoxanthin. (H) Stratification vs. nitrate : silicate in surface water. (I) Stratification vs. light attenuation coefficient. Correlations that are not indicated by a line are not significant, $p > 0.10$.

plankton show the opposite response, namely an increase in abundance with temperature (Fig. 7F).

Bacterioplankton anomalies—The evidence of multiyear change also appears in other ecosystem variables. The optical environment has been changing markedly (Fig. 4I) with a strong negative correlation to stratification (Fig. 5I). Much of the light attenuation can be ascribed to the phytoplankton itself, since a rank correlation between Chl *a* and the extinction coefficient is extremely significant ($\tau = 0.85$, $p < 0.01$). However, it is reasonable to assume that a portion of the attenuation is also due to heterotrophic bacterioplankton (Fig. 6I), which changes coherently with phytoplankton biomass at the interannual scale (Fig. 7G).

Deep seston anomalies—The amount of phytoplankton material detected near the bottom of the basin at 60 m is tightly linked to surface concentrations of Chl *a* (Fig. 7H). On an annual average basis, the concentration of deep POC is 29% that of surface POC, indicating that a substantial portion of seston sinks and remains unremineralized for delivery to the benthic system. Deep POC has been decreasing since 2002, coincident with intensified stratification and lower diatom concentration. Although the negative correlation of deep POC with stratification is not statistically significant (Fig. 7I, Table 1), it is a weak result based on only 4 yr of data.

Mesozooplankton anomalies—The dominant mesozooplankton in Bedford Basin are copepods: *Pseudocalanus minutus, Oithona similis, Acartia clausi, Temora longicornis, and Eurytemora herdmani*. Our 5-yr weekly records (Fig. 8A–C) indicate maximum abundance in late summer (Fig. 8D–F) and no statistical evidence of interannual linkage to their presumptive food source (Fig. 8G–I, Table 1).

Discussion

The question of how phytoplankton at coastal sites around the world are responding to ongoing global change (Smetacek and Cloern 2008) is one of the most pressing in

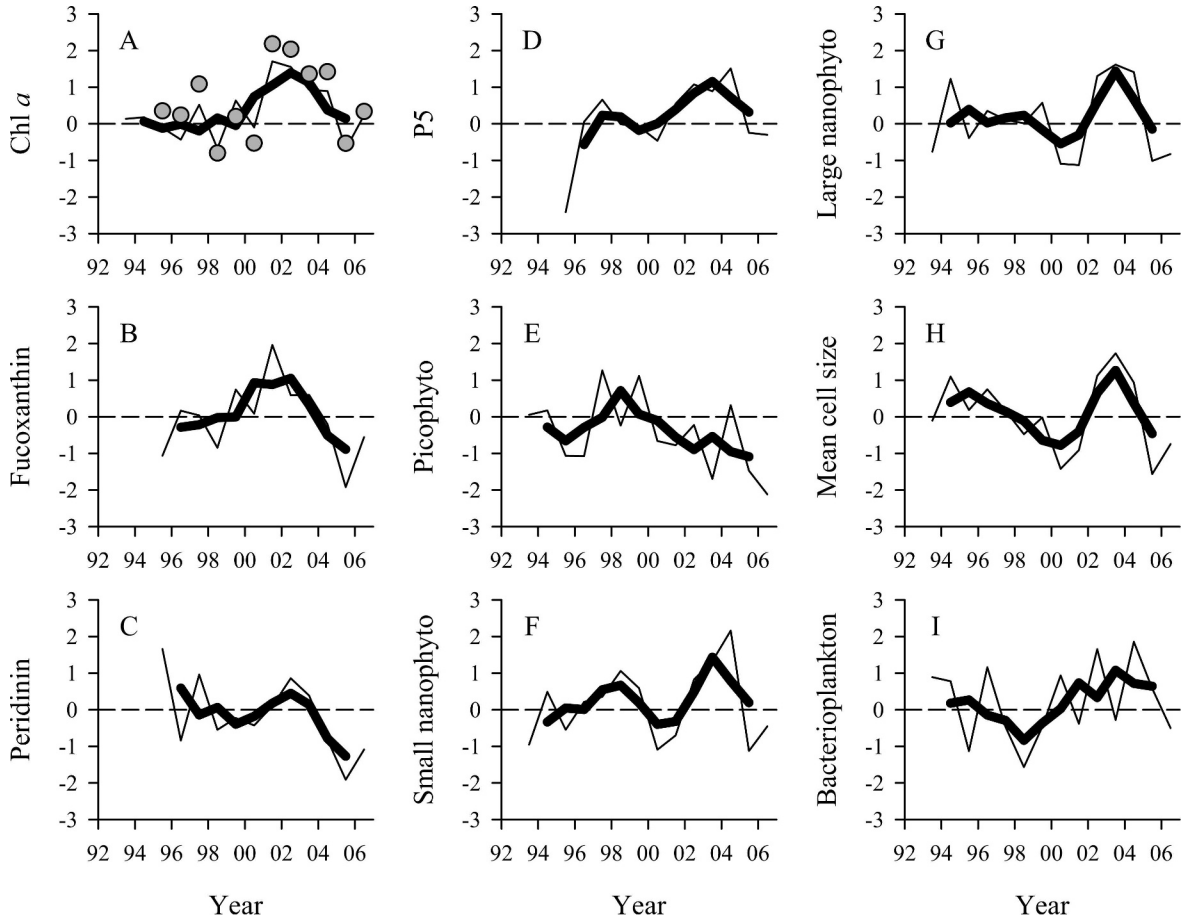

Fig. 6. Time series of pigment and microbial concentrations. (A) Chl *a*, lines indicate measurement by fluorometer, circles indicate measurement by HPLC (log mg m^{-3}). (B) Fucoxanthin (log mg m^{-3}). (C) Peridinin (log mg m^{-3}). (D) P5, *see* Methods (log mg m^{-3}). (E) Picophytoplankton (log mg C m^{-3}). (F) Small nanophytoplankton (log mg C m^{-3}). (G) Large nanophytoplankton (log mg C m^{-3}). (H) Assemblage mean cell size ESD (μm). (I) Bacterioplankton (log cells ml^{-1}). Lines as in Fig. 2.

contemporary marine ecosystem science. As the timescale of phytoplankton population dynamics is on the order of weeks, the answer must be sought from trends arising from high-frequency monitoring of annual cycles over many years (Li 2007). The most tractable approach remains the description of direction, magnitude, and frequency of departures from long-term mean conditions in both climate and ecosystem components, for the purpose of detecting common patterns (McGowan 1990). Fourteen years of weekly observations in Bedford Basin provide adequate scope (Schneider 2001) for an analysis of phytoplankton trends in relation to variations in atmospheric and hydrospheric conditions. Other long-term coastal data sets have addressed complex interactions leading to observed phytoplankton change (Smetacek and Cloern 2008), but few studies are opportune to document conditions before, during, and after the passage of a multiyear signal. The sustained period of positive salinity anomaly from 1998 to 2004 (Fig. 4G) in Bedford Basin was a natural experiment that we use here to empirically verify two general predictive constructs of how phytoplankton respond to climate change: indirectly through stratification and directly through temperature.

Vertical stratification of the water column strongly shapes the structure of phytoplankton communities and is the basis upon which general predictions (Doney 2006) and specific predictions from computer models (Sarmiento et al. 2004) are made concerning the effects of a warmer climate on phytoplankton. Essentially, under conditions of limiting nutrient flux from deep source water to the surface illuminated layer, further stratification due to increasing temperature (Behrenfeld et al. 2006) or decreasing salinity (Chiba et al. 2004) in the upper layer is predicted to reduce phytoplankton. In this circumstance, species that rely on well-mixed high nutrient conditions to counteract low cellular surface-to-volume ratio and negative passive buoyancy would not be favored (Cullen et al. 2002). Many of these species are diatoms in the microplankton size fraction. Indeed, highly stratified waters are dominated by picoplankton, whereas well-mixed waters contain a more evenly distributed mix of phytoplankton size classes (Li 2002). Prevailing concepts relating turbulence and nutrients to phytoplankton life forms (Cullen et al. 2002) are implicitly based on proximate considerations such as cellular strategies of nutrient acquisition, buoyancy, and pigment packaging. Thus, the appropriate timescale is

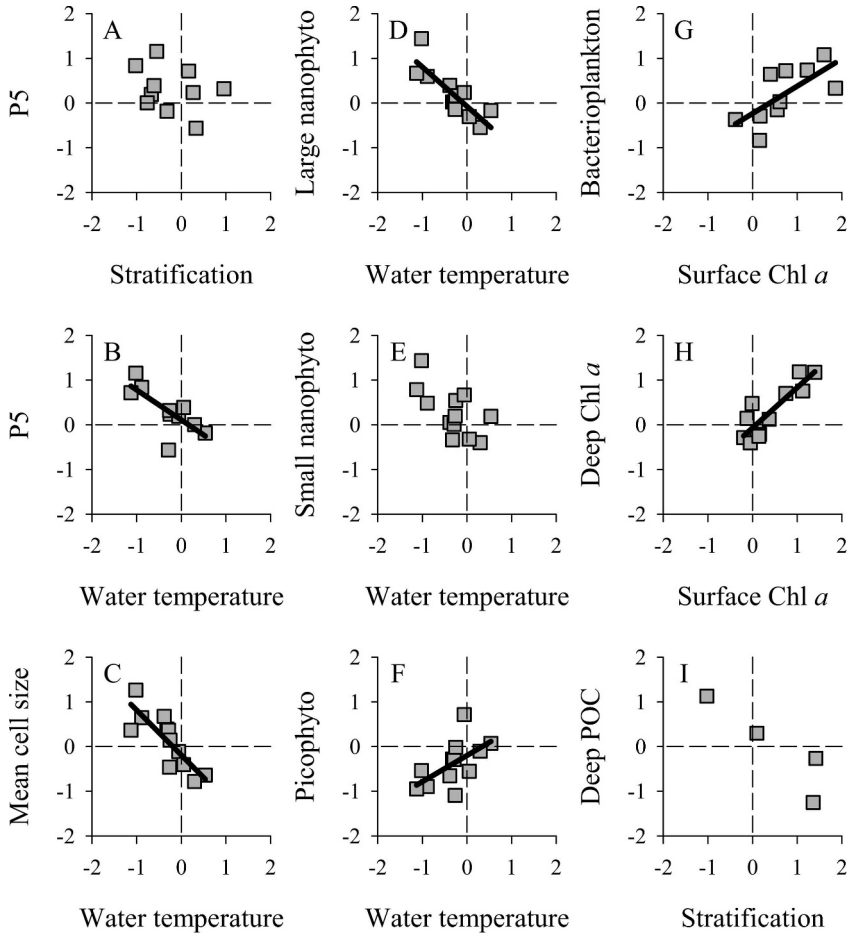

Fig. 7. Rank correlations of normalized annual anomalies. (A) Stratification vs. P5. (B) Water temperature vs. P5. (C) Water temperature vs. mean cell size of combined nanophytoplankton and picophytoplankton assemblage. (D) Water temperature vs. large nanophytoplankton carbon. (E) Water temperature vs. small nanophytoplankton carbon. (F) Water temperature vs. picophytoplankton carbon. (G) Surface Chl *a* vs. bacterioplankton. (H) Surface Chl *a* vs. deep Chl *a*. (I) Stratification vs. deep POC. Correlations that are not indicated by a line are not significant, $p > 0.10$.

seasonal or shorter. In Bedford Basin, as in many other temperate bodies of water, the control of stratification by temperature within the course of a year is clear (Fig. 1E). This is the basis for blooms in spring (low temperature, weak stratification) of diatoms, and blooms in late summer (high temperature, strong stratification) of small flagellated phytoplankters.

On the other hand, the appropriate timescale for predicting the effects of climate change is interannual. In Bedford Basin, there is no statistical link between annual changes in temperature and stratification (Fig. 5D). Temperature has a strong seasonal cycle, but yearly averages are not very different. On the other hand, salinity has a weak seasonal cycle, but yearly averages are substantially different. It was as if the temperature cycle is reset to a somewhat similar level every year, whereas the salinity cycle is nudged higher or lower. Thus, at the interannual scale, changes in stratification are related to changes in salinity (Fig. 5C). This is also generally true over the adjoining Scotian Shelf and Gulf of Maine, but lower-salinity water in this broader region has an upstream origin from the Labrador Current and the St. Lawrence estuary. Notably, in these shelf waters, reduced freshening was also recorded from 1999 to 2004, correlating with a delay in the onset of the spring phytoplankton bloom (Ji et al. 2007).

In Bedford Basin, the biological response during years of below-normal stratification is clear: phytoplankton as a whole (Fig. 5F), and those containing fucoxanthin in particular (Fig. 5G), are at above-normal concentrations, leaving a high ratio of residual nitrate : silicate (Fig. 5H). A strong atmospheric driver (air temperature) can propagate to parts of the ecosystem (diatoms) through connections that have weak intra-annual variability (salinity) rather than strong intra-annual variability (water temperature). This outcome, though consistent with our understanding of seasonal dynamics, is remote from mechanisms at the cellular and population levels. Instead, the outcome is more appropriately viewed as a macroscopic result related in principle to the net summation of all processes that transpire over a year. As such, it is empirical evidence that

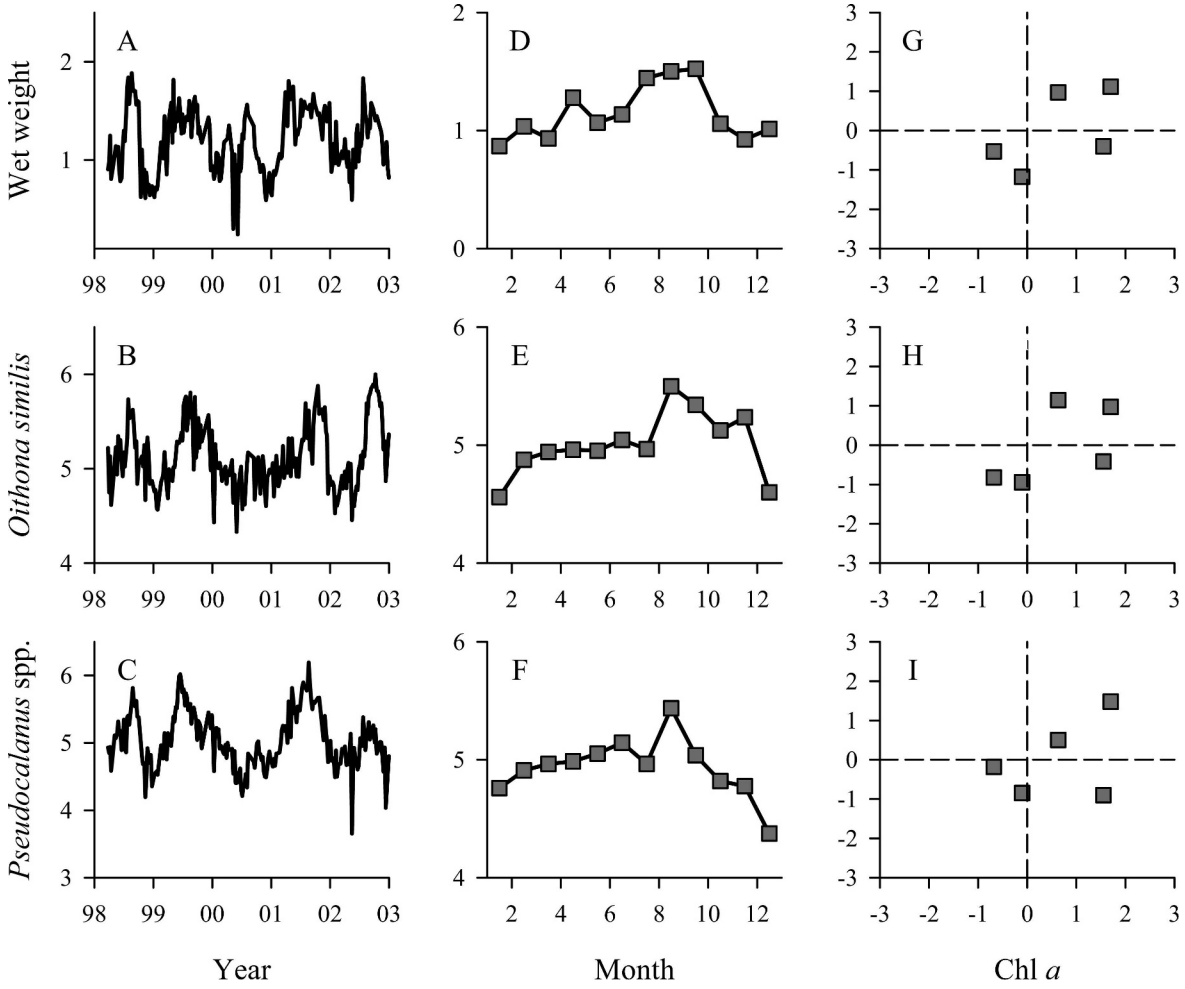

Fig. 8. (A–C) Copepod time series, (D–F) annual cycles from multiyear observations averaged into monthly bins, and (G–I) rank correlations with Chl *a* for (A,D,G) total wet weight in units of log g m^{-2}, (B,E,H) *Oithona similis* in units of log individual m^{-2}, and (C,F,I) *Pseudocalanus* spp. in units of log individual m^{-2}.

stratification remains an important determinant of phytoplankton structure even when scaled up to the interannual level away from proximate control. This affirms an underlying premise in atmosphere–ocean-coupled climate models that examine ecosystem response.

An alternative approach for predicting phytoplankton response to long-term environmental change is to make observations in diverse ecosystems across a broad spatial scale, testing for statistical links between biological phenomena and environmental predictors. Here, the intercomparison of mean states across different systems is used to infer a possible change in state of one particular system. Whether or not it is the same to sample many independent realizations of a process as to observe the process for a long time is an untested assumption in marine ecology (Frank et al. 2008). Notwithstanding this uncertainty, there is a similitude in the way that picophytoplankton abundance is positively related to temperature encountered in diverse ecosystems (Li 2008), and the way that picophytoplankton abundance increases with temperature on an annual average basis in Bedford Basin (Fig. 7F). A first-order explanation for this pattern can be proposed (X. A. G. Morán, Á. López-Urrutia, A. Calvo-Díaz, and W. K. W. Li unpubl.) on the basis of macroecological relationships between organism size, temperature, and abundance (Atkinson et al. 2003; White et al. 2007). The positive correlation between annual anomalies of picophytoplankton and temperature in Bedford Basin is consistent with this interpretation, but the contrasting results for nanophytoplankton (Fig. 7D,E) require another explanation, which we do not have. In a climate of rising temperature, the net outcome of these opposite responses from different size classes is an emphatic shift toward a community of lower-standing biomass (Fig. 7B) with a lower mean assemblage cell size (Fig. 7C). In this way, it is remarkable that the interannual community pattern over time resembles the pattern across diverse ecosystems (Bouman et al. 2003) and also the pattern across protist taxonomic categories (Atkinson et al. 2003).

The means by which interannual variability in physical drivers is transmuted to phytoplankton lie in a complex

array of interacting hierarchical mechanisms that start from molecular synthesis and lead to recruitment of specific populations and thence to assembly of community structures (Reynolds 2002). However, not only do plankton respond to climatic signals through the dominant environmental variables, they can also respond through trophic interactions to subtle climatic signals that are spread across different meteorological variables (Taylor et al. 2002). For example, atmospherically driven changes in ocean currents have been shown to intensify a trophic cascade, leading to increased phytoplankton in San Francisco Bay (Cloern et al. 2007). On the Scotian Shelf offshore from Bedford Basin, there is also a reported trophic cascade that apparently relieves grazing pressure on the phytoplankton (Frank et al. 2005), but this is a continental shelf scale interdecadal phenomenon ascribed to the removal of top predators. At the local interannual scale of Bedford Basin, there is no statistically significant evidence of negative correlation between copepods and phytoplankton that would indicate top-down control (Fig. 8, Table 1). Conversely, bottom-up control on most of the dominant copepods cannot be easily rejected in view of the positive but weak rank correlations with phytoplankton. In contrast, the trophic link from phytoplankton to heterotrophic bacterioplankton is strongly evident in Bedford Basin (Fig. 7G). This coherent variation of microbial primary and secondary producers has also been established over the much larger regions of the Scotian Shelf and the Labrador Sea (Li et al 2006*a*). Further, it now seems that an empirical link can be made from changes in the euphotic zone to the aphotic zone (Fig. 7H). It follows that increased stratification might be associated with decreased seston at depth (Fig. 7I), indicating a propagation of the atmospheric signal to the sea floor.

The body of evidence here that links changes in the atmosphere, the water, the phytoplankton, the bacterioplankton, and the seston is entirely correlative. The assignment of causation is therefore inferential. Each individual correlation provides only weak inference, but there is stronger support when the sequence of individual correlations is compounded from driver to the primary responder and thence to secondary responders. Direct observation and correlative statistics are the foundation of pattern recognition, and climate change creates the natural experiments that test the robustness of these patterns (Kerr et al. 2007). In experimental ecology, the environment is purposefully manipulated from one state to another to elicit a predicted biological response. In observational ecology, the environment is changed by natural forcing, first one way (e.g., cooling) and then the other way (e.g., warming). If the biological response also changes, first one way (e.g., decrease abundance) and then the other way (e.g., increase abundance), the likelihood of causation from alternative agents is greatly reduced. This coherent ''sign switching'' contributes to a diagnostic fingerprint of climate change (Parmesan and Yohe 2003) and discredits the dyslogism often attached to the correlative approach.

Temporal sign switching is clearly indicated in Bedford Basin. Statistically, the strongest evidence ($\tau > |0.7|$) is the change in diatom (fucoxanthin) concentration with stratification, and the change in community composition (assemblage ESD) with temperature. These results suggest that in a warming climate, there may be an inreasing importance of small phytoplankton with a consequent reduction in export production. Empirical verification will depend on sustained long-term monitoring with sufficient temporal resolution.

References

Atkinson, D., B. J. Ciotti, and D. J. S. Montagnes. 2003. Protists decrease in size linearly with temperature: *ca*. 2.5% $^{\circ}C^{-1}$. Proc. R. Soc. Lond. B **270:** 2605–2611.

Behrenfeld, M. J., and others. 2006. Climate-driven trends in contemporary ocean productivity. Nature **444:** 752–755.

Bouman, H. A., and others. 2003. Temperature as indicator of optical properties and community structure of marine phytoplankton: Implications for remote sensing. Mar. Ecol. Prog. Ser. **258:** 19–30.

Chiba, S., T. Ono, K. Tadokoro, T. Midorikawa, and T. Saino. 2004. Increased stratification and decreased lower trophic level productivity in the Oyashio region of the North Pacific: A 30-year retrospective study. J. Oceanogr. **60:** 149–162.

Claustre, H. 1994. The trophic status of various oceanic provinces as revealed by phytoplankton pigment signatures. Limnol. Oceanogr. **39:** 1206–1210.

Cloern, J. E. 2001. Our evolving conceptual model of the coastal eutrophication problem. Mar. Ecol. Prog. Ser. **210:** 223–253.

———, A. D. Jassby, J. K. Thompson, and K. A. Hieb. 2007. A cold phase of the East Pacific triggers new phytoplankton blooms in San Francisco Bay. Proc. Natl. Acad. Sci. USA **104:** 18561–18565.

Cullen, J. J., W. F. Doolittle, S. A. Levin, and W. K. W. Li. 2007. Patterns and prediction in microbial oceanography. Oceanography **20:** 34–46.

———, P. J. S. Franks, D. M. Karl, and A. Longhurst. 2002. Physical influences on marine ecosystem dynamics, p. 297–336. *In* A. R. Robinson, J. J. McCarthy and B. J. Rothschild [eds.], The sea. V. 12. Wiley.

Doney, S. C. 2006. Plankton in a warmer world. Nature **444:** 695–696.

Frank, K. T., J. A. Fisher, and W. C. Leggett. 2008. Macroecological analysis of temporal change in aquatic ecosystems: Progress and outlook, Paper 3592. *In* W. K. W. Li and P. A. del Giorgio [conveners], Macroecological perspectives on long term change in aquatic ecosystems, American Society of Limnology and Oceanography. Annual meeting, St. John's, Newfoundland, Canada.

———, B. Petrie, J. S. Choi, and W. C. Leggett. 2005. Trophic cascades in a formerly cod-dominated ecosystem. Science **308:** 1621–1623.

Gregory, D., B. Petrie, F. Jordan, and P. Langille. 1993. Oceanographic, geographic and hydrological properties of Scotia-Fundy and southern Gulf of St. Lawrence inlets. Can. Tech. Rep. Hydrogr. Ocean Sci. **143:** 1–248.

Hughes, S. L. and N. P. Holliday [eds.] 2007. ICES Report on Ocean Climate 2006. International Council for the Exploration of the Sea Cooperative Research Report No. 289. 55 p.

Hurrell, J. W., and R. R. Dickson. 2004. Climate variability over the North Atlantic, p. 15–31. *In* N. R. Stenseth and G. Ottersen [eds.], Marine ecosystems and climate variation: The North Atlantic, a comparative perspective. Oxford Univ. Press.

Jeffrey, S. W., and M. Vesk. 1997. Introduction to marine phytoplankton and their pigment signatures, p. 37–84. *In* S. W. Jeffrey, R. F. C. Mantoura and S. W. Wright [eds.], Phytoplankton pigments in oceanography: Guidelines to modern methods, United Nations Educational, Scientific, and Cultural Organization,

Ji, R., C. S. Davis, C. Chen, D. W. Townsend, D. G. Mountain, and R. C. Beardsley. 2007. Influence of ocean freshening on shelf phytoplankton dynamics. Geophys. Res. Lett. **34:** L24607, doi:10.1029/2007GL032010.

Kerr, J. T., H. M. Kharouba, and D. J. Currie. 2007. The macroecological contribution to global change solutions. Science **316:** 1581–1584.

Lewis, M. R., and T. Platt. 1982. Scales of varaibility in estuarine ecosystems, p. 3–20. *In* V. S. Kennedy [ed.], Estuarine comparisons. Academic.

Li, W. K. W. 2002. Macroecological patterns of phytoplankton in the northwestern North Atlantic Ocean. Nature **419:** 154–157.

———. 2007. Macroscopic patterns in marine plankton. Encyclopedia of biodiversity. Elsevier. doi:10.1016/B978-012226865-6/00582-1.

———. In press. Plankton populations and communities. *In* J. D. Witman and K. Roy [eds.], Marine macroecology. Univ. of Chicago Press.

———, and P. M. Dickie. 2001. Monitoring phytoplankton, bacterioplankton, and virioplankton in a coastal inlet (Bedford Basin) by flow cytometry. Cytometry **44:** 236–246.

———, W. G. Harrison, and E. J. H. Head. 2006*a*. Coherent sign switching in multiyear trends of microbial plankton. Science **311:** 1157–1160.

———, ———, and ———. 2006*b*. Coherent assembly of phytoplankton communities in diverse temperate ocean ecosystems. Proc. R. Soc. B **273:** 1953–1960.

Longhurst, A. 1995. Seasonal cycles of pelagic production and consumption. Prog. Oceanogr. **36:** 77–167.

McGowan, J. A. 1990. Climate and change in oceanic ecosystems: The value of time-series data. Trends Ecol. Evol. **5:** 293–299.

Miller, W. D., and L. W. Harding Jr. 2007. Climate forcing of the spring bloom in Chesapeake Bay. Mar. Ecol. Prog. Ser. **331:** 11–22.

Mitchell, M. R., G. Harrison, K. Pauley, A. Gagné, G. Maillet, and P. Strain. 2002. Atlantic zonal monitoring program sampling protocol. Can. Tech. Rep. Hydrogr. Ocean Sci. **223:** 1–23.

Parmesan, C., and G. Yohe. 2003. A globally coherent fingerprint of climate change impacts across natural systems. Nature **421:** 37–42.

Petrie, B., and P. Yeats. 1990. Simple models of the circulation, dissolved metals, suspended solids and nutrients in Halifax Harbour. Water Poll. Res. J. Can. **25:** 325–349.

Reynolds, C. S. 2002. On the interannual variability in phytoplankton production in freshwaters, p. 187–221. *In* P. J. Le, B. Williams, D. N. Thomas and C. S. Reynolds [eds.], Phytoplankton productivity: Carbon assimilation in marine and freshwater ecosystems. Blackwell.

Richardson, A. J., and D. S. Schoeman. 2004. Climate impact on plankton ecosystems in the Northeast Atlantic. Science **305:** 1609–1612.

Sarmiento, J. L., and others. 2004. Response of ocean ecosystems to climate warming. Global Biogeochem. Cycles, **18:** GB3003, doi:10.1029/2003GB002134.

Schneider, D. C. 2001. Scale, concept and effects of, p. 245–254. *In* S. A. Levin [ed.], Encyclopedia of biodiversity, V. 5. Academic Press.

Smayda, T. J., D. G. Borkman, G. Beaugrand, and A. Belgrano. 2004. Responses of marine phytoplankton populations to fluctuations in marine climate, p. 49–58. *In* N. R. Stenseth and G. Ottersen [eds.], Marine ecosystems and climate variation: The North Atlantic, a comparative perspective. Oxford Univ. Press.

Smetacek, V., and J. E. Cloern. 2008. On phytoplankton trends. Science **319:** 1346–1348.

Sokal, R. R., and F. J. Rohlf. 1995. Biometry, 3rd ed. Freeman.

Taylor, A. H., J. I. Allen, and P. A. Clark. 2002. Extraction of a weak climatic signal by an ecosystem. Nature **416:** 629–632.

Uitz, J., H. Claustre, A. Morel, and S. B. Hooker. 2006. Vertical distribution of phytoplankton communities in open ocean: An assessment based on surface chlorophyll. J. Geophys. Res. **111:** C08005, doi:10.1029/2005JC003207.

Verity, P. G., C. Y. Robertson, C. R. Tronzo, M. G. Andrews, J. R. Nelson, and M. E. Sieracki. 1992. Relationships between cell volume and the carbon and nitrogen content of marine photosynthetic nanoplankton. Limnol. Oceanogr. **37:** 1434–1446.

White, E. P., S. K. Morgan Ernest, A. J. Kerkhoff, and B. J. Enquist. 2007. Relationships between body size and abundance in ecology. Trends Ecol. Evol. **22:** 323–330.

Received: 4 December 2007
Accepted: 22 April 2008
Amended: 29 April 2008